Quasi-Elastic Scattering of 160-MeV Protons by Alpha Clusters in Light Nuclei. I. Carbon*

B. Gottschalk
Northeastern University, Boston, Massachusetts 02115

and

S. L. Kannenberg
Northeastern University, Boston, Massachusetts 02115 and Boston State College, Boston, Massachusetts 02115

(Received 5 December 1969)

α-cluster knockout from Be^9, C^{12}, and O^{16} by 160-MeV protons was investigated. The outgoing proton and α particle were detected in coincidence and their momenta measured with good resolution. Knockout, sequential decay, and spallation reactions were observed. Proton and α detection angles were varied so as to test the plane-wave impulse-approximation (PWIA) model of the knockout reaction over a wide range of the effective p-cluster interaction. The method, apparatus, and carbon results are discussed in this paper. Measured values of the fully differential cross section $(d\sigma/d\Omega_\alpha d\Omega_p dT_p)$ are given, and are shown to vary nearly as predicted by the PWIA. The errors due to finite detector sizes (finite momentum resolution) are discussed in some detail. The recoil correction to the usual PWIA expression for the cross section is derived. The branching ratio to the first excited state of the residual Be^8 nucleus, as well as the effective number of α clusters in C^{12}, are discussed and compared with theoretical predictions.

One reaction that occurs when light nuclei are bombarded with medium-energy protons is the quasi-elastic scattering of the incident particle by α-particle clusters in the nucleus. If both the scattered proton and the recoiling cluster emerge with sufficient energy, they may be detected in coincidence and their momenta may be measured. It is then possible to calculate the binding energy and initial momentum of the cluster in the target nucleus for each observed event, if one assumes that no "secondary" interactions occurred between the incoming and/or outgoing particles and the residual nucleus. Thus the probability of finding the target nucleus in various (core + α-particle) states, as well as the momentum distribution of the α particle in each of these states, can be measured. The validity of this interpretation depends, of course, on precisely how serious the effects of secondary interactions are, how well the p-cluster interaction inside a nucleus can be approximated by the free p-α interaction, and similar questions.

The qualitative value of this "quasi-elastic" or "knockout" picture of the reaction is well established by experiment. Samman and Cuer[1] obtained direct evidence of it (1958) in photographic emulsions. They observed many events where one of the α particles from the reaction

$$p + C^{12} \rightarrow p' + 3\alpha \text{ (180 and 360 MeV)}$$

had considerably more energy than the other two; these events were interpreted as the direct knockout of an α particle from carbon followed by the breakup, into two more α particles, of the residual Be^8 nucleus. The first experiment using counters was that of James and Pugh[2] in 1963, on the same reaction with 150-MeV incident protons. They detected the outgoing proton and α particle in coincidence, inferring the cluster momentum distribution from the dependence of the measured cross section upon the α-particle detection angle. Another counter experiment at medium energies was performed by Ruhla *et al.*[3] on Li^6 and Be^9. Yuasa and Hourani[4] have obtained bubble-chamber data on the reaction in carbon at 85 MeV. Recently, Roos *et al.*[5] have shown that the knockout model provides a consistent interpretation of $Be^9(p,p\alpha)$ data even at 57 MeV; however, the reaction in carbon at this energy appears[6] to be dominated by other mechanisms.

We have mentioned only "fully differential" measurements in which the parameters of the final state are, at least in principle, completely measured. There have also been many experiments in which only one outgoing particle was detected, which are also susceptible to a knockout interpretation; the most recent of these are the (p, α) experiments of Komarov, Kosarev, and Sauchenko[7] at 665 MeV.

Much theoretical effort has also been devoted to the knockout model. Jackson[8] has pointed out the formal difficulties in justifying this model for

cluster reactions (noting, however, that the requirements are best met for the relatively stable α cluster). She has also suggested[9] a specific form (to permit certain simplifying approximations) for $(p,p\alpha)$ experiments designed to investigate clustering in light nuclei. Balashov, Boyarkina, and Rotter[10] have predicted excitation spectra of residual nuclei and α-cluster momentum distributions, using parentage coefficients calculated from the shell model and neglecting secondary interactions. Beregi *et al.*,[11] also starting from the shell-model description of the target nucleus, have calculated the "effective number of α clusters" available for knockout in various nuclei. Sakamoto[12] has calculated the angular correlations expected in $(p,p\alpha)$ reactions also using a knockout model without secondary interactions; his formulas are evaluated at the rather low incident energy 30–50 MeV.

No single calculation, however, has brought together *all* the aspects of the problem which appear to be important: The formation of clusters from the independent-particle states of the target nucleus, the effective p-cluster interaction inside the nucleus, and finally the localization of the interaction and the distortion of outgoing waves by absorption and refraction. Theoretical effort on this difficult problem might be stimulated if, as in the $(p,2p)$ case,[13] it could be shown that the simplest theoretical description, the plane-wave impulse approximation (PWIA), already gives fairly good account of the measured cross sections. Specifically, one can calculate a "distorted momentum distribution" $P(q)$ from the measured cross sections using the PWIA. If the PWIA were exact, $P(q)$ for α particles in a given state of a given nucleus would be found to be the same in all conceivable medium-energy knockout experiments, involving different incident energies, different incident particles, and/or different final-state configurations. Any change in $P(q)$ as these parameters are varied is a measure of the breakdown of the PWIA, and may also provide some clue as to what kinds of distortion dominate, and therefore what approach theory should take. Although highly desirable, the comparison of α-knockout experiments with different incident energies or even with different incident particles obviously involves a very long-range experimental program. Fortunately, the many degrees of freedom in the three-body final state provide ample opportunity for checking the consistency of the PWIA, even at a single incident energy, and this is what we have done. The same philosophy motivated the recent experiments of Roos *et al.*[5]

We have studied the $(p,p\alpha)$ reaction at 160 MeV in Be^9, C^{12}, and O^{16}, observing several different final-state configurations in each case. The distorted momentum distributions for each nucleus appear to depend surprisingly little on the strength of the effective p-α interaction, but do depend somewhat on scattering angles and/or outgoing particle energies, suggesting that "refraction" distortions may dominate as in the $(p,2p)$ case.[13] The over-all consistency of PWIA is sufficiently good that it should be possible to reconstruct the "true" momentum distributions and parentage coefficients with a distorted-wave theory. Measurements at several different incident energies are probably necessary to determine the effect of absorption, so that the measured "effective number of α clusters" [being sensitive also to any distortions of the *shape* of $P(q)$] must be interpreted very cautiously. The present paper will discuss the design of the experiment and details of the apparatus and procedure, as well as the carbon results; a second paper will present the beryllium and oxygen results.

I. DESIGN OF THE EXPERIMENT

A. Kinematic Considerations

Suppose a nucleus is bombarded by medium-energy protons and an outgoing proton and α particle are detected in coincidence; let us assume that the undetected residual nucleus of mass M does not break up during the interaction time. Let T stand for a kinetic energy, $\vec{k}$ for a wave number, and the subscripts 0, p and α for the incident proton, the outgoing proton, and the α particle, respectively. Then energy-momentum conservation requires

$$T_0 = T_p + T_\alpha + T_r + E_b\,, \tag{1a}$$

$$\vec{k}_0 = \vec{k}_p + \vec{k}_\alpha + \vec{q}\,, \tag{1b}$$

where

$$T_r = [(\hbar q c)^2 + (Mc^2)^2]^{1/2} - Mc^2 \tag{2}$$

is the kinetic energy of the recoiling residual nucleus, small but not negligible, and $\vec{q}$ is its wave vector. E_b is the net loss of kinetic energy in the reaction and, if the α particle is emitted in its ground state, is related to the excitation E_x of the residual nucleus by

$$E_b = E_x - Q_m\,, \tag{3}$$

where Q_m is the Q value of the reaction.

Setting E_b and q equal to zero in Eqs. (1), one obtains the elastic p-α scattering case, in which the specification of the outgoing proton angles (for

instance) determines the remaining final-state variables (α momentum and proton energy). This still holds true if E_b is allowed some moderate nonzero value; the angle of the outgoing α particle relative to the outgoing proton is then a few degrees smaller. We call this the "quasifree" case[14] and the corresponding proton/α angle settings for a given E_b, the "quasifree configurations." These are coplanar and will be denoted as θ_p/θ_α for brevity; for instance, 62/50 means "the coplanar configuration $\theta_p = 62°$, $\theta_\alpha = 50°$" (angles measured to the beam line).

If q is not necessarily zero, we need to specify (in addition to E_b and the outgoing proton direction) three more quantities to determine the final state; let these be the proton kinetic energy T_p and the α direction. $\vec{q}$ and T_α can then be found by solving Eqs. (1) and (2). The sum $T_p + T_\alpha$ is almost constant, since T_r is small [Eq. (1)]. The range of possible values of q at a given configuration will include $q = 0$ if, and only if, it is a quasifree configuration. In this experiment four different quasifree configurations were investigated; q is plotted as a function of T_p for each one in Fig. 1(a), assuming the typical case $E_b = 7.4$ MeV and $Mc^2 = 7454$ MeV (knockout of an α cluster from carbon, leaving the residual Be^8 nucleus in its ground state). The region between the dashed lines, determined by the minimum and maximum α-particle energies (12 and 100 MeV) accepted by the apparatus, was probed in the experiment. We will define T_{qf} as that value of T_p for which $q = 0$ in a given configuration.

In applying the knockout formula, it is also necessary to know the momentum transfer to the α cluster, since the effective p-cluster interaction depends strongly upon it. In the knockout model, where $-\hbar\vec{q}$ is interpreted as the initial laboratory momentum of the α cluster, the momentum transfer is $\hbar\vec{k}$ where $\vec{k} = \vec{k}_\alpha + \vec{q}$; k is plotted in analogous fashion to q in Fig. 1(b).

In using the knockout model to obtain k, which we then use to determine the effective interaction in "checking" the knockout model, we are indulging in circular reasoning. Indeed, we remark once and for all that our experiment merely demonstrates the self-consistency of this model, and does not preclude some other explanation.

B. Competing Reactions

Some of the considerations in this and the following sections have already been stated by James and Pugh[2] and Roos *et al.*[5] We have repeated them in order to present a complete discussion.

At least three mechanisms can lead to p-α

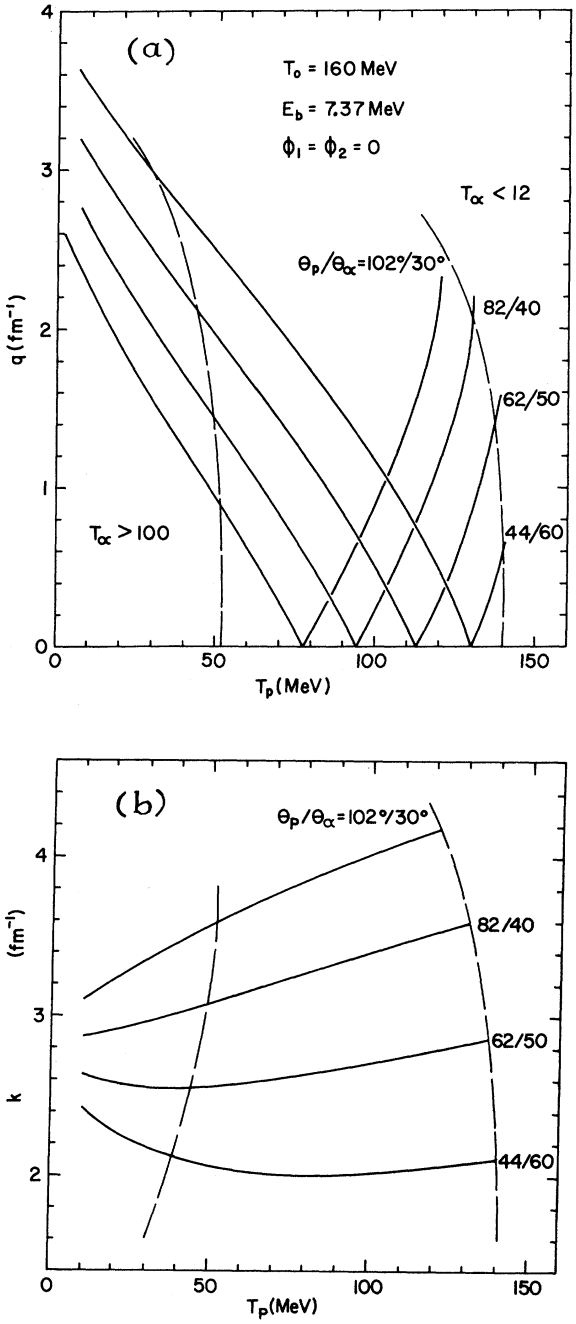

FIG. 1. Kinematic relations relevant to the experiment: (a) Recoil momentum $|q|$ of the residual nucleus as a function of proton energy T_p, at four "quasifree" settings of the proton and α counters; (b) momentum transfer to the α particle as a function of T_p, at the same settings. Calculations are for coplanar reactions with $T_0 = 160$ MeV, $E_b = 7.37$ MeV, mass of residual nucleus = 8. The regions to the left of the first dashed line and to the right of the second dashed line indicate the experimental cutoffs due, respectively, to the α energy being too great or too small.

coincidences; for example, with a carbon target

$$p + C^{12} \rightarrow p' + \alpha + Be^8 \qquad \text{(knockout)} \qquad (4a)$$

$$\rightarrow p' + C^{12*} \searrow \alpha + Be^8 \qquad \begin{pmatrix}\text{sequential}\\ \text{decay}\end{pmatrix} \qquad (4b)$$

$$\rightarrow p' + \alpha + \text{other particles (spallation)}. \qquad (4c)$$

Spallation is likely to yield rather low-energy α particles and protons, only weakly correlated in angle and energy, since the final state has four or more particles. Sequential decay, however, leads to a three-body final state which is kinematically indistinguishable from knockout. However, if the excitation of the carbon nucleus is great, many decay modes will be possible, and α decay will occur only in a fraction of these. That is, the higher the energy of the α particles detected in the experiment, the less likely are they to arise from the decay of well-defined states of C^{12}, which might strongly affect the cross section. At high enough incident energy it should always be possible to select configurations yielding α particles of high enough energy to be attributed to knockout. The T_p, T_α correlation plots (Fig. 6) obtained at 160 MeV show that sequential decay and knockout are well separated at two of the configurations we used.

C. Plane-Wave Impulse Approximation

In the Born approximation, the fully differential cross section for scattering a proton from a cluster of mass number a bound in a target nucleus of mass number A in a state characterized by the binding energy E_b is

$$\left.\frac{d\sigma}{d\Omega_\alpha d\Omega_p dT_p}\right|_{E_b} = \frac{m}{\hbar^2}\,\frac{(1+a)^2}{a}\,\frac{k_p k_\alpha}{k_0} \times f \times \left(\left.\frac{d\sigma}{d\Omega}\right|_{p\alpha,\text{c.m.}}\right) P(q), \qquad (5)$$

with

$$f = \left(1 - \frac{a}{A}\right)\left[1 + \frac{a}{A}\left(\frac{k_p}{k_\alpha}\cos(\theta_p + \theta_\alpha) - \frac{k_0}{k_\alpha}\cos\theta_\alpha\right)\right]^{-1}$$

in our geometry. $P(q)$ is the probability density distribution of the cluster momentum relative to the residual nucleus. A derivation of Eq. (5) is given in the Appendix. As A becomes large $f \rightarrow 1$, and Eq. (5) reduces to the formula given, for instance, by Riou.[15] However, this approximation (the neglect of recoil effects in the kinematic factor) is not warranted in the present experiment, as f varies between 0.85 and 1.20 over the region of interest.

According to Eq. (5) the measured cross section should vary as the product of three factors:

(1) The probability of finding in the target nucleus a cluster of the appropriate momentum to yield the observed reaction.

(2) The "strength" $d\sigma/d\Omega$ (in the p-cluster c.m. frame) of the primary p-cluster interaction.

(3) A slowly varying kinematic factor which relates experiments with different incident energies, final-state configurations, etc. This factor accounts for the volume of $\vec{q}$ space sampled in a particular experiment.

Some drastic approximations are made in deriving Eq. (5):

(1) Total disregard of how such a cluster might arise in the first place; questions of antisymmetrization of nucleon wave functions, etc., are simply not considered. (James and Pugh[2] speak of "preformed" α clusters.)

(2) Neglect of secondary interactions between the residual "core" and the proton or α particle.

(3) Neglect of any off-energy-shell effects in the p-cluster interaction, arising from the binding of the cluster in the nucleus.

Thus we bypass all the problems of nuclear structure, but hopefully account for all the "kine-

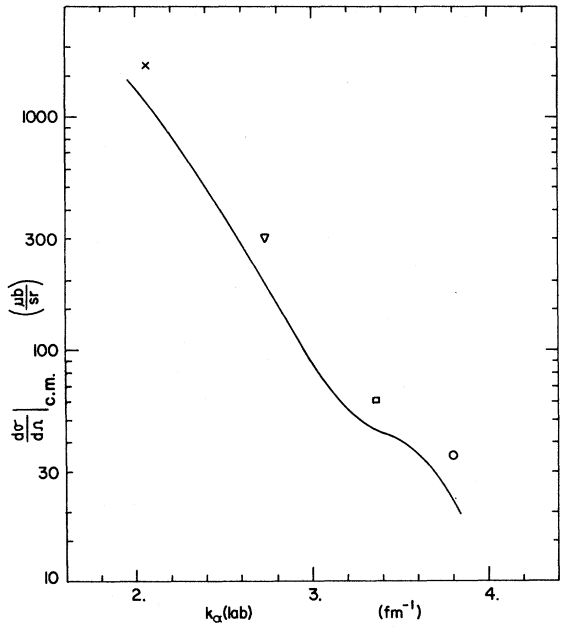

FIG. 2. Free p-α cross section in the c.m. system as a function of momentum transfer, after Cormack *et al.*[16] The symbols indicate typical momentum transfers encountered at each quasifree configuration used in the present experiment.

matic" features of the reaction.

The elastic p-α cross section has been measured at 147 MeV by Cormack *et al.*,[16] who also showed that elastic p-α scattering is a function mainly of the momentum transfer to the α particle, over a wide range of incident energies. Figure 2 shows $d\sigma/d\Omega(p\alpha, \text{c.m.})$ as a function of momentum transfer calculated from Cormack's data, along with symbols indicating typical momentum transfers encountered in each of the configurations we used; the cross section varies by a factor 55 over this range, so that a good test of at least one aspect of Eq. (5) is possible.

II. EXPERIMENTAL ARRANGEMENT AND PROCEDURE

Figure 3 is a schematic diagram of the experimental arrangement. The unpolarized proton beam of the Harvard cyclotron was focused to a spot about 0.64 cm high and 1.0 cm wide, full-width at half-maximum flux at the target position. It was stochastically extracted for a duty cycle of about 20%, neglecting rf time structure (which did not affect the experiment). The beam was reduced in intensity using a slit at the extraction channel entrance, which also reduced the energy spread. A helium-filled ionization chamber upstream of the target monitored the beam; the monitor had been tested for saturation and calibrated against a scintillation counter counting full-energy protons at the target position. The beam energy was 159.4 MeV by range in CH_2.[17] The beam intensity, limited by pulse pileups in the proton detector, was typically 1×10^{10} proton/sec.

The target was a 9.87-mg/cm^2 CH_2 foil mounted with the α telescope in a vacuum chamber; it was always set facing the α counters to minimize energy losses. Over-all energy resolution was limited by the beam quality and the proton counter except at low energies of the α particle, where the uncertainty introduced by the target thickness was as great as 4 MeV.

The proton detector was a 7.64×7.64-cm NaI(Tl) crystal[18] behind a brass collimator which defined the solid angle. The collimator was 3.8 cm thick and had a 1.9-cm-diam hole; its rear face was 27.6 cm from the target. The α telescope comprised a brass collimator followed by a thin "passing" counter followed by a "stopping" counter. The collimator was 3.8 cm deep, had a 0.95-cm-diam hole, and its rear face was 19.0 cm from the target. The passing counter was a totally depleted 106-μ transmission-mounted silicon surface-barrier detector.[19] The stopping counter was a 4-mm-deep lithium-drifted silicon detector.[20] 12-MeV α particles from the target reached the stopping detector, and α particles up to 100 MeV stopped in it; these numbers determined the acceptance of the experiment as shown in Fig. 1(a).

The T_p, ΔT_α, and T_α signals were sent to the counting room by charge-sensitive preamplifiers. Here, all three signals were processed identically by homemade circuits: first, a double-delay-line amplifier produced a bipolar pulse to reduce rate effects. Then, a discriminator viewing this pulse generated a timing signal at zero crossing. The

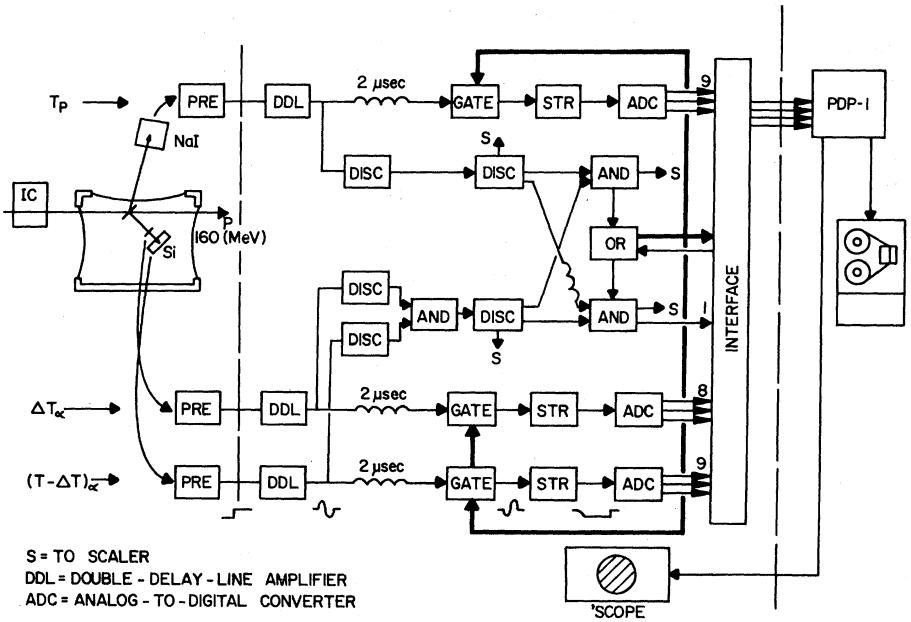

FIG. 3. Block diagram of the experimental arrangement.

bias was normally set at 20-MeV equivalent for the proton, threshold for T_α, and just high enough to reject high-energy protons in ΔT_α. Commercial fast-logic units were then used to determine an "α" coincidence between T_α and ΔT_α, which in turn was put in coincidence with both "prompt" and "delayed" (three cyclotron rf periods) versions of the T_p discriminator output. Either a "prompt" or a "delayed" coincidence initiated the analysis of an event so that the spectrum of chance coincidences was sampled continuously. The proton-α resolving time [full width at half maximum (FWHM) of the relative delay curve] was 90 nsec.

The analog signals were stored in 2-μsec delay lines to compensate for delays in the discriminators and fast logic; whenever a coincidence "trigger" occurred, these signals were gated, stretched, digitized, and transmitted to the computer. Thus for each "event" 9 bits of T_p data, 9 of T_α data, 8 of ΔT_α data, and one prompt/delayed identification bit were ultimately recorded on magnetic tape for subsequent analysis. The time-shared PDP-1 provided useful diagnostic information during the run (single-counter pulse-height spectra, energy-correlation "scatter plots," etc.), but there was no on-line particle identification, sorting, or rejection of events. Instead, the final magnetic tape was a verbatim list of the pulse heights associated with each event accepted by the fast-logic and discriminator criteria.

Some *RC* filtering (~0.5-μsec time constant) look place in the amplifier subsequent to time pickoff and prior to gating, significantly reducing the noise in the ΔT_α channel and improving the particle identification. The over-all performance of the system will be discussed with the data analysis.

The proton-α coincidence circuit was crudely timed on free p-p coincidences from the CH_2 and later checked with helium in the vacuum chamber. Particle-identification stability was periodically checked by removing the proton-coincidence requirement; in subsequent analysis no change in the relation between ΔT_α and T_α with time was observed. Energy calibration of all counters was accomplished by observing free p-α scattering with 1 atm of helium in the scattering chamber, at five different angular settings; this procedure was repeated at the end of the run. About two weeks were spent accumulating the carbon data; each angular configuration was divided into at least two blocks widely separated in time, and configurations with low rates (such as 102/30) were interspersed with high-rate configurations (such as 44/60) to check the stability of the counters. At the end of the run the beam profile was measured by the darkening of glass slides, calibrated by means of several exposures of different durations. These profile data were necessary to estimate the resolution effect of finite beam size, and to estimate the small counting losses due to the beam spot being, unfortunately, comparable in size to the hole in the α collimator.

III. DATA ANALYSIS AND RESULTS

A. Particle Identification

Events from $(p,p\mathrm{He}^3)$ reactions cannot contaminate the $(p,p\alpha)$ events populating the ground and first excited states of Be^8 which will be discussed below, because of the large Q value of the $(p,p\mathrm{He}^3)$ reaction. However, since a future paper will take up the $(p,p\mathrm{He}^3)$ events, we will outline the particle identification procedure here, in order to complete our description of the data analysis.

Figure 4(a) shows the correlation of T_α and ΔT_α pulse heights associated with p-α coincidences. The doubly charged ion group is subdivided into He^3 and He^4 groups. There are a few points due to a triply charged group, a few due to "fold-over" (particles passing through the T_α counter), and a few which cannot readily be accounted for, presumably due to poor charge collection, pileup, etc.

The analysis program identified the particle in the "α arm" for each event as follows: (a) Assuming the particle was an α particle, it calculated the *expected* energy loss in the ΔT counter using the observed energy loss in the T counter, the range-energy relation in silicon, and the known thickness of the ΔT counter; (b) it calculated the percentage discrepancy Δ between the expected and observed energy losses in ΔT; and (c) it accepted the particle as an α particle if $-9\% < \Delta < +15\%$. Figure 4(b) is a typical distribution of Δ for a subgroup of particles which deposited 30 to 50 MeV in the stopping counters, showing the cuts used by the analysis program. Using large batches of data obtained by temporarily removing the p coincidence requirement, the particle separation was studied as a function of particle energy; the energy calibration of the ΔT counter was then adjusted by a few percent to permit using the same cuts for all observed energies. (The required adjustment was too small to affect subsequent E_b and q calculations.)

B. Detector Calibrations and Energy Resolution

The detectors were calibrated by filling the target chamber with helium at 1 atm and collecting elastic p-α events at five angles. Figure 5(a)

shows the proton-α energy correlation for four of these angles. The "tails" are due to nuclear interactions of the proton in the NaI. The proton calibration was checked in the direct beam with CH_2 absorbers. Using the analysis program, the proton and α calibrations were adjusted to give a peak centered at $E_b = 0$ for the elastic events. The final energy-calibration function of each detector was linear (pulse height versus energy deposited in counter). A typical elastic E_b peak is shown in Fig. 5(b); the linewidth of 2 MeV FWHM is typical of the actual experiment since all effects except target thickness (which was important only for low-energy α particles) are included.

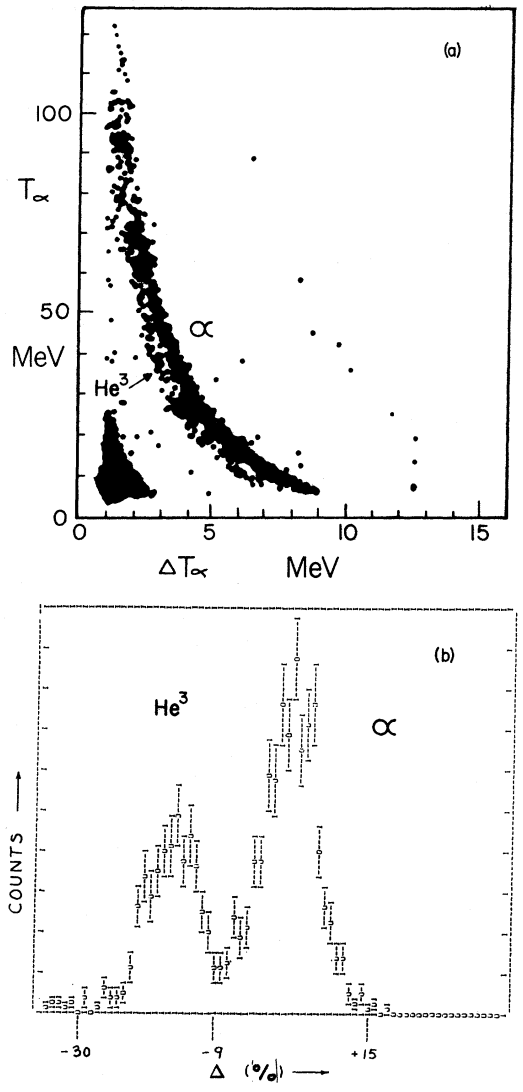

FIG. 4. (a) Scatter plot of the energy loss ΔT in the front α counter versus the particle energy T, for about 1900 coincident events. (b) Typical distribution (found by the analysis program) of the percentage discrepancy between ΔT measured and ΔT expected on the assumption that the particle was an α. Particles with energies between 30 and 50 MeV are included; this distribution is best regarded as a "slice" of the doubly charged ion group of (a). The cuts used by the analysis program to identify He^4 and He^3 ions are shown.

Long-term drifts in the proton counter had been minimized by the use of a charge-sensitive preamplifier, permitting operation at low average phototube currents. A study of the E_b peaks obtained in the carbon run showed no drift after the first two days. Addition of a remote target changer for the second (oxygen and beryllium) run permitted daily stability checks using elastic p-α scattering; this is a useful safeguard.

The over-all residual uncertainty in E_b due to drift and calibration errors is ±0.5 MeV.

C. Data Analysis Program

The Harvard IBM 7094 computer analyzed each event as follows: (a) Pulse heights were converted to energies using the calibration functions determined by elastic scattering; (b) the particle in

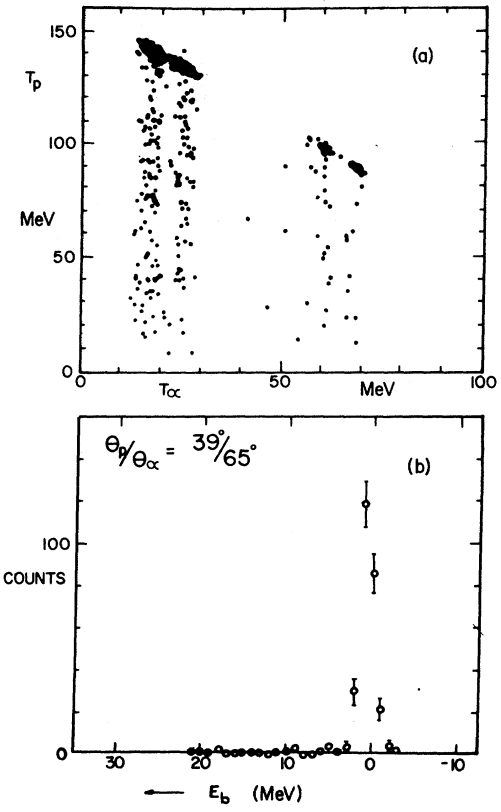

FIG. 5. Free p-α calibrations and energy resolution. (a) Scatter plot of T_p versus T_α for four free p-α configurations used to calibrate the detectors. The vertical "tails" are caused by nuclear interactions of the proton in the NaI crystal. (b) Distribution of the sum of proton and α-particle energies for one of the configurations.

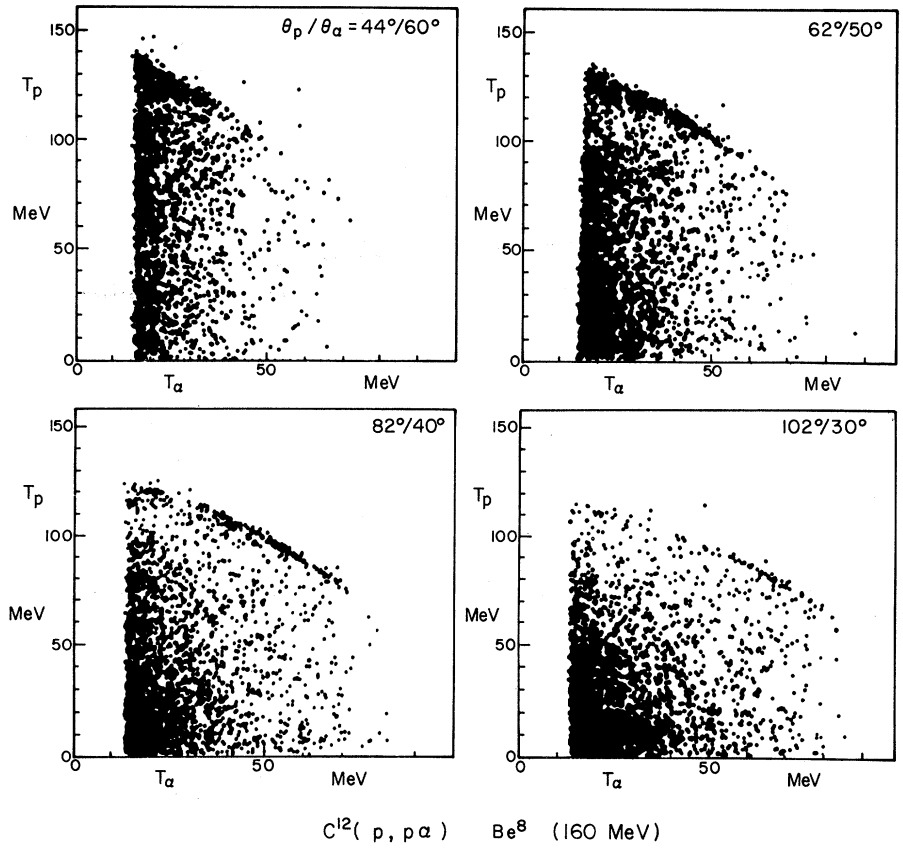

FIG. 6. Scatter plots of proton energy T_p versus α energy T_α for coincident events at four quasifree configurations. The three-body kinematic line, corresponding to the reaction $C^{12}(p,p\alpha)Be^8$ (160 MeV) with the residual Be^8 nucleus in its ground or first excited state, is clearly seen in each case. In the third and fourth cases, the contributions to this line from sequential decay and knockout are well separated. The contribution of chance coincidences has not been subtracted, and is thus seen to be small in the quasi-elastic region.

the α arm was identified as α, He^3, or "other" as described above, and its energy found by adding T and ΔT; (c) both particle energies were corrected for the average loss in the target; (d) the recoil momentum $\hbar q$ of the residual nucleus was found by momentum closure [Eq. (1a)]; and (e) the binding energy E_b was calculated [Eqs. (2) and (1b)]. The event was then classified according to a "He^3 or α" index, a "prompt" or "delayed" index, T_p (5-MeV channels), and E_b (1-MeV channels). After processing each run, the computer prepared "particle separation" distributions [Fig. 4(b)], E_b distributions of events in selected T_p ranges, and tables of cross sections and $P(q)$ values for events in any desired E_b and T_p ranges. These tables facilitated comparison of data subgroups.

Figure 6, the T_p/T_α correlation of events identified as $(p,p\alpha)$, shows that the events we shall discuss belong to a well-defined group. The 82/40 data, especially, show a clear separation of knockout, sequential decay (upper left-hand

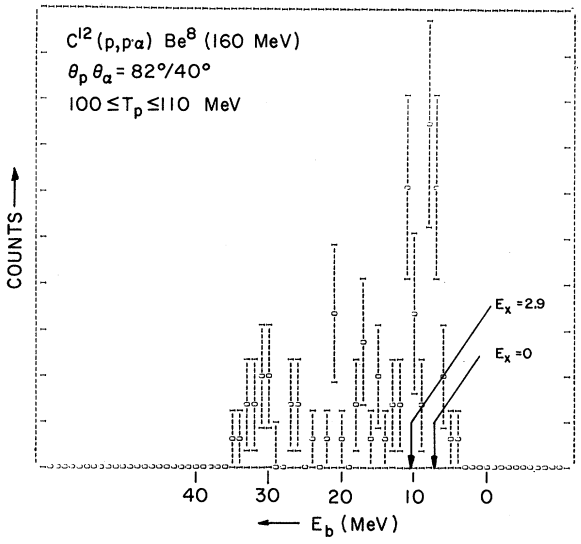

FIG. 7. A typical binding-energy spectrum (produced by the analysis program) for events with $q \cong 0$.

(corner), and spallation events. Knockout and sequential decay are not resolved at 44/60 and 62/50 where $q=0$ corresponds to a lower α energy. The contribution of chance coincidences has *not* been subtracted in Fig. 6 and is thus seen to be very small in the knockout region (even though it was 30% averaged over all particles and energies). It was of course formally subtracted in the data analysis.

Figure 7 is a typical E_b distribution (82/40 data with $T_p \cong T_{qf}$). Most of the E_b distributions show clear evidence of the 2.9-MeV excited state of Be^8.

IV. RESULTS AND DISCUSSION

A. Momentum-Resolution Effects

In coincidence experiments of this sort it is usual to take

$$\text{measured cross section} = \frac{C}{D}\,\frac{1}{\Delta\Omega_\alpha \Delta\Omega_p \Delta T_p}\,. \tag{6}$$

C is the observed number of counts; the factor D includes the number of incident protons, the target nuclei/cm^2, and in our case a slowly varying correction for nuclear absorption in the sodium iodide detector. $\Delta\Omega_\alpha$ and $\Delta\Omega_p$ are the α- and proton-detector solid angles, and ΔT_p is the proton energy bin width (5 MeV) used in the data analysis. Equation (6) is valid if doubling $\Delta\Omega_\alpha$ (for instance) would in fact double the observed counts. This will not happen, however, if the outgoing proton and α momenta are significantly correlated within the "phase-space region" defined by $\Delta\Omega_\alpha$, $\Delta\Omega_p$, and ΔT_p. One need only think of the limiting case of free proton-α scattering where, given a small proton counter, an α counter of whatever size would register the same number of coincidences. It is obvious that, even in the present less extreme case, the correlation will *lower* the measured cross section [as defined by Eq. (6)] relative to its true value. (This statement assumes that proton and α pairs coming near the centers of their respective counters are *more* probable; if *less* probable, as with a p-state momentum distribution, the measured cross section will be spuriously *high*.)

A finite beam spot size leads to a similar error, since protons in the periphery of the beam spot, though counted equally by the beam monitor, are less effective in producing coincidences, because of the correlations. In fact, the experimental factors contributing to this error in the cross section are the very same factors which limit the ability of the apparatus to resolve the vector $\vec{q}$. These factors, which flatten maxima and fill in minima in the cross sections measured in knockout experiments, have been recognized qualitatively in the knockout literature but have not been well estimated quantitatively.[21] In particular, it is misleading simply to estimate the uncertainty in q and indicate it by a horizontal error bar in the distorted momentum distribution, since this ignores the related *systematic* error in the cross section, as well as a systematic shift in the q value itself, as we shall show.

By numerical methods it is possible to estimate both the uncertainty in q at each point and the magnitude of what might be called the "finite-detector" effect on the measured cross section. As so often happens, one cannot actually correct the data for this effect, but one can see whether the measured momentum distribution $P_m(q)$ is consistent with an assumed "test" distribution $P_t(q)$ (which might be supplied by theory) by calculating how the experimental configuration and data-analysis procedure would distort[22] P_t. The counts observed in the experiment are related to the true differential cross section by

$$C = D\int_{\Delta\Omega_\alpha}\int_{\Delta\Omega_p}\int_{\Delta T_p}\left(\frac{d\sigma}{d\Omega_\alpha d\Omega_p dT_p}\right) d\Omega_\alpha d\Omega_p dT_p\,,$$

where the integrations span the experimental detector sizes and bin widths. The "true" differential cross section in the integrand is assumed to be related to the test momentum distribution by Eq. (5), so that

$$C = D\int_{\Delta\Omega_\alpha}\int_{\Delta\Omega_p}\int_{\Delta T_p} (\text{kinematic factor}) \times\frac{d\sigma}{d\Omega}(k) P_t(q) d\Omega_\alpha d\Omega_p dT_p\,. \tag{7}$$

The momentum transfer $\vec{k}$ and the initial momentum $\vec{q}$ of the α particle are functions of the independent variables θ_α, φ_α, θ_p, φ_p, and T_p, and the kinematic factor varies slowly with these variables. Having observed this number of counts, we say we have measured [according to Eq. (5)]

$$P_m(q') = (\text{measured cross section}) \times \frac{1}{(\text{kin. factor})\times\frac{d\sigma}{d\Omega}(k')}$$

or, using Eqs. (6) and (7)

$$P_m(q') = \frac{1}{d\sigma(k')/d\Omega}\,\frac{1}{\Delta\Omega_\alpha\Delta\Omega_p\Delta T_p}\int_{\Delta\Omega_\alpha}\int_{\Delta\Omega_p}\int_{\Delta T_p}\frac{d\sigma}{d\Omega}(k) \times P_t(q) d\Omega_\alpha d\Omega_p dT_p\,.$$

Here q' and k' are suitable "effective values" (to

be discussed) of k and q. If, as must be done in practice, the integral is evaluated numerically, for instance by means of a Monte Carlo calculation of N throws, we obtain

$$P_m(q') = \frac{1}{d\sigma(k')/d\Omega} \frac{1}{N} \sum_{I=1}^{N} \frac{d\sigma}{d\Omega}(k_I) P_t(q_I),$$

where $\vec{k}_I$ and $\vec{q}_I$ are the values obtained in the ith throw of the independent variables. Experimental effects such as finite beam size and constraints such as collimators can be included in an obvious way; we do not attempt to write down a rigorous formal expression. We emphasize that N is the *total* number of throws; it is precisely those terms in the sum which lead to small values of $P_t(q_I)$ or which are "killed" by the collimator that cause the expected lowering of $P_m(q)$ relative to $P_t(q)$.

Using such a program, we have estimated these effects in the present experiment. Angular divergence of the beam was neglected, but the finite beam spot size was included by weighting each spot on the target by the local flux as found from the glass-slide measurements. Values of θ_α, φ_α, θ_p, and φ_p were chosen so as to cover each detector (defined by the rear face of the corresponding collimator) uniformly. Events were weighed with 0 if the α particle hit the front edge of its collimator; in this way the small counting losses mentioned at the end of Sec. II were calculated. The test distribution was a Gaussian with a half width at half maximum of 0.325 fm^{-1} following Balashov[10] (though his curve is not exactly Gaussian). Various tests with this program showed that:

(a) The choice of $d\sigma(k_I)/d\Omega$ in Eq. (8) had little effect. Accordingly, we approximated it by a simple exponential function of k, and took for the effective value k', the nominal value.

(b) Events where the α particle hit the front edge of the collimator had only slightly greater average q than events which were counted. Therefore, this problem only caused a small over-all reduction in the measured absolute cross section[23] at each angular setting, without affecting the shape of $P(q)$.

(c) The mean and mode (most likely) values of q for each experimental bin were, near small q values, systematically larger than the nominal value for that bin. At large q, the difference becomes insignificant. The nominal and most likely values are shown for comparison in the table. This effect is easily understood; even though the experimental parameters are tuned exactly to $q = 0$, q is always positive and the experimental parameters vary over finite ranges and, therefore, the average q is always greater than zero. In the present case, an additional contribution to this unavoidable shift came from a slight asymmetry of the beam flux about the target center; this contribution was included. The important conclusion here, which applies qualitatively to any knockout experiment done with finite counters, is that there exists a region near $q = 0$ which one is *not* in fact probing with the experiment, and which gets wider as the experimental resolution gets worse.

(d) The previous source of shift in the effective q value of each bin is purely "experimental" in nature; another potential source is the variation of $P_t(q)$ itself across the bin. This turned out to be small even for the rather sharp Gaussian we assumed; that is, the mean value of q for successive throws in a given bin depended relatively little on whether these were weighted with $P_t(q)$ or not. This is fortunate, since otherwise the data analysis would be unavoidably coupled to the theoretical predictions.

We obtained the following numerical results for our experimental conditions: Assuming the true $P(q)$ were a Gaussian with a half width of 0.325 fm^{-1} at half maximum, the measured cross section as defined by Eq. (6) would be 30% lower than the true differential cross section near $q = 0$.[24] The correction falls off with increasing q, reaching 14% at $q = 0.6$ fm^{-1}. It is a similar function of q for all four telescope settings.

B. Cross Sections and Distorted Momentum Distributions

The foregoing discussion shows that it is permissible to continue using the "naive" formula (6) in our data analysis, provided we plot each datum at the "most likely" q value as given by the Monte Carlo program, rather than at the nominal q value. We must then remember to calculate, by means of the Monte Carlo technique, the experimental distortion of any given theoretical prediction before comparing it with our results. Thus we choose to stop our "data analysis" short of attempting to correct for the finite-counter effects, since to do that would require knowing the true $P(q)$.

Experimental results are presented in the table and in Figs. 8 and 9. The table lists the differential cross sections [calculated according to Eq. (6)] as a function of T_p for the four quasifree configurations investigated. Data for the ground ($3.5 \leq E_b \leq 9.0$ MeV) and first excited ($9.0 < E_b \leq 13.5$ MeV) states of the residual Be^8 nucleus are given separately. We have corrected for nuclear interactions of the proton in the sodium iodide detector.[25] Errors are statistical standard devia-

tions, and the over-all normalization error is negligible by comparison. Figure 8 is a graph of these cross sections, with the points corresponding to each set of angles connected by straight lines to guide the eye. The change in the order of magnitude of the cross section from one configuration to the next (see also Fig. 2) and the fact that each curve peaks near T_{qf} already show that a quasi-elastic mechanism dominates, certainly for the ground-state events. The secondary rise of the cross section at large T_p (small T_α) due to sequential-decay reactions is not resolved at

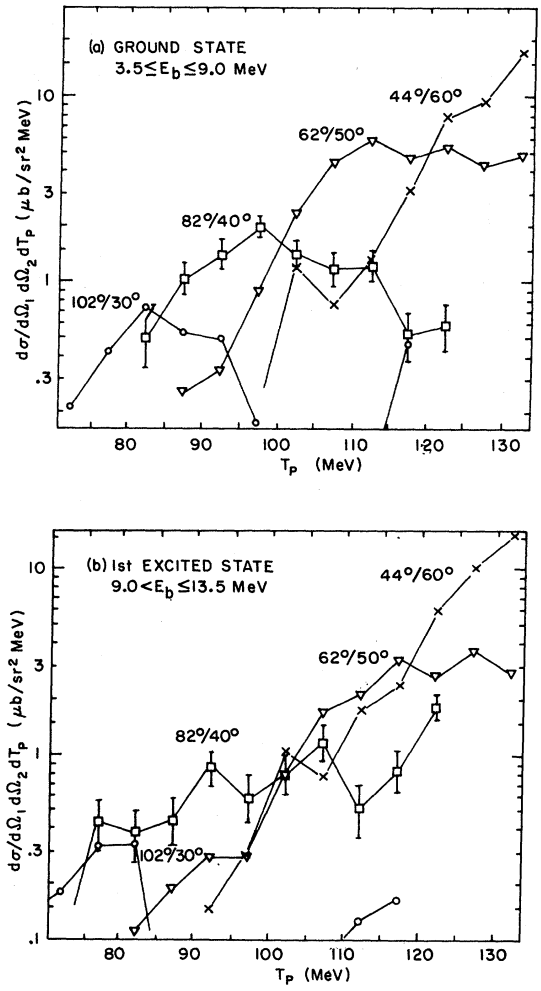

FIG. 8. Differential cross sections as a function of T_p for the reaction $C^{12}(p,p\alpha)Be^8$ (160 MeV), for events populating the (a) ground and (b) first excited states of Be^8. The symbols along the bottom indicate the expected position of the maximum cross section at each configuration, according to the knockout model. The secondary rise at large T_p in the 82/40 and 102/30 cases is due to sequential-decay reactions. Errors are statistical standard deviations; the over-all normalization error is small by comparison.

44/60 and 62/50, as was already clear from Fig. 6.

Column 4 of the table lists $P(q)$ calculated from the cross sections of column 3, using Eq. (5) with the free p-α cross sections measured by Cormack *et al.* (Ref. 16 and Fig. 2). Column 5 lists the nominal q value for each case and column 6 the mode or "most likely" q assignment. This was calculated as described in the previous section. It is insensitive to the assumed "true" momentum distribution and differs appreciably from the nominal value only at small q.

Figure 9 shows the distorted momentum distributions (columns 4 and 6 of the table) of α clusters in C^{12}. These appear to be quite different for clusters coupled to the ground and first excited states of Be^8. In the former case, the four configurations combine to form quite a consistent picture of $P(q)$, especially in view of the wide variation in the strength of the effective p-α cross section. The picture for the first-excited-state events is much more confused. This qualitative

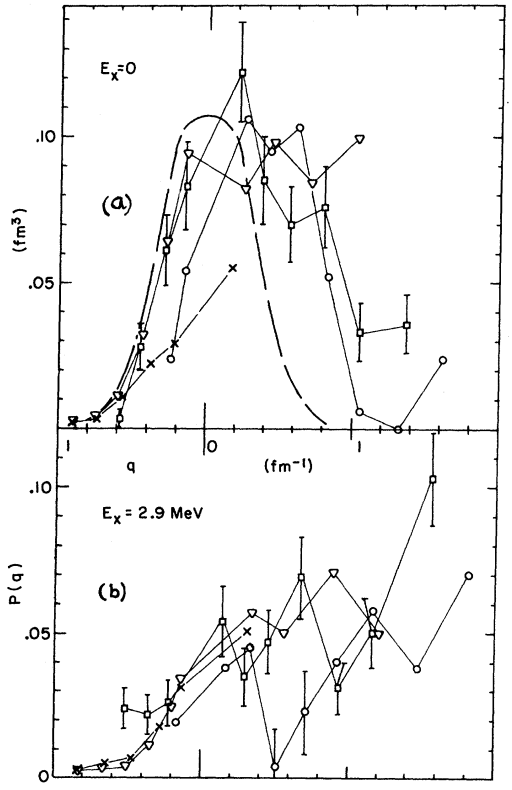

FIG. 9. Distorted momentum distributions $P(q)$ of the α clusters in C^{12} coupled to (a) the ground, and (b) first excited states of Be^8. These are calculated from the measured cross sections (Fig. 8) using the PWIA [Eq. (5)]. The dashed curve represents the prediction of Balashov *et al.* (Ref. 9), arbitrarily normalized and corrected for experimental momentum resolution effects.

TABLE I. Measured values of the fully differential cross section $d\sigma/d\Omega_\alpha d\Omega_p dT_p$ for knockout of α clusters in C^{12} by 160-MeV protons, the residual nucleus being left in its (A) ground, or (B) first excited state. Column 1, the telescope angles given as θ_p/θ_α; column 2, the central value of the proton kinetic energy in each bin; column 3, the cross section and its statistical standard deviation; column 4, the calculated value of the distorted momentum distribution [Eq. (5)]; column 5, the nominal q value for the corresponding T_p; and column 6, the most likely q value for that bin when experimental resolution effects are taken into account by a Monte Carlo calculation. Entries in column 3 were corrected for nuclear absorption of the proton in the NaI detector, but not for the lowering effect of finite detector sizes. The over-all normalization error is small compared to the statistical errors.

θ_p/θ_α	$\langle T_p \rangle$ (Mev)	$\frac{d\sigma}{d\Omega_\alpha d\Omega_p dT_p}$ (μb/sr^2 MeV)	$P(q)\times 100$ (fm^3)	Nominal q (fm^{-1})	Most likely q (fm^{-1})
(A)		Events populating Be^8 ground state, $3.5 \leq E_b < 9.0$ MeV			
44°/60°	107.5	0.7 ±0.3	0.20 ±0.09	0.89	0.91
	112.5	1.3 ±0.4	0.34 ±0.12	0.72	0.74
(× on	117.5	4.1 ±0.8	1.1 ±0.2	0.54	0.56
	122.5	7.7 ±1.1	2.2 ±0.3	0.35	0.37
graphs)	127.5	9.5 ±1.2	2.9 ±0.4	0.13	0.21
	132.5	17.3 ±1.7	5.5 ±0.5	0.12	0.18
62°/50°	87.5	0.25 ±0.1	0.28 ±0.13	0.88	0.90
	92.5	0.33 ±0.1	0.40 ±0.16	0.73	0.75
(▽ on	97.5	0.90 ±0.2	1.1 ±0.3	0.56	0.59
	102.5	2.4 ±0.4	3.2 ±0.5	0.39	0.43
graphs)	107.5	4.4 ±0.5	6.4 ±0.7	0.21	0.27
	112.5	5.8 ±0.6	9.4 ±0.9	0.02	0.14
	117.5	4.7 ±0.5	8.2 ±0.9	0.19	0.25
	122.5	5.3 ±0.6	9.8 ±1.	0.42	0.45
	127.5	4.3 ±0.5	8.4 ±1.	0.69	0.71
	132.5	4.8 ±0.5	9.9 ±1.	1.03	1.03
82°/40°	77.5	0.06 ±0.05	0.34 ±0.28	0.56	0.58
	82.5	0.50 ±0.1	2.8 ±0.8	0.40	0.44
(□ on	87.5	1.0 ±0.2	6.1 ±1.2	0.23	0.28
	92.5	1.4 ±0.2	8.3 ±1.5	0.05	0.14
graphs)	97.5	2.0 ±0.3	12.2 ±1.7	0.14	0.22
	102.5	1.4 ±0.2	8.5 ±1.5	0.33	0.38
	107.5	1.2 ±0.2	7.0 ±1.3	0.55	0.57
	112.5	1.2 ±0.2	7.6 ±1.4	0.78	0.80
	117.5	0.53 ±0.15	3.3 ±1.0	1.05	1.05
	122.5	0.58 ±0.16	3.6 ±1.0	1.37	1.37
102°/30°	72.5	0.23 ±0.1	2.4 ±1.0	0.16	0.23
	77.5	0.47 ±0.16	5.4 ±1.8	0.02	0.14
(○ on	82.5	0.80 ±0.19	10.6 ±2.6	0.20	0.27
	87.5	0.59 ±0.17	9.5 ±2.7	0.39	0.43
graphs)	92.5	0.50 ±0.15	10.3 ±3.0	0.59	0.62
	97.5	0.18 ±0.09	5.2 ±2.6	0.81	0.83
	102.5	0.02 ±0.07	0.6 ±2.0	1.04	1.06
	107.5	0 ± ...	0 ±...	1.30	1.31
	112.5	0.09 ±0.06	2.4 ±1.7	1.61	1.62
	117.5	0.48 ±0.15	11.8 ±3.6	2.00	...
(B)		Events populating Be^8 first excited state, $9.0 \leq E_b \leq 13.5$ MeV			
44°/60°	107.5	0.75 ±0.33	0.20 ±0.09	0.81	0.83
	112.5	1.7 ±0.5	0.48 ±0.14	0.64	0.65
	117.5	2.3 ±0.6	0.66 ±0.17	0.45	0.47
	122.5	5.8 ±0.9	1.76 ±0.28	0.24	0.28
	127.5	9.8 ±1.2	3.12 ±0.4	0.02	0.14
	132.5	15.0 ±1.5	5.07 ±0.5	0.27	0.31
62°/50°	87.5	0.19 ±0.13	0.23 ±0.15	0.81	0.83
	92.5	0.28 ±0.12	0.34 ±0.15	0.65	0.67
	97.5	0.28 ±0.14	0.37 ±0.18	0.49	0.51
	102.5	0.79 ±0.22	1.1 ±0.3	0.31	0.35

TABLE I (*Continued*)

θ_p/θ_α	$\langle T_p \rangle$ (MeV)	$\frac{d\sigma}{d\Omega_\alpha d\Omega_p dT_p}$ (μb/sr^2 MeV)	$P(q)\times 100$ (fm^3)	Nominal q (fm^{-1})	Most likely q (fm^{-1})
	107.5	1.7 ±0.3	2.5 ±0.5	0.12	0.20
	112.5	2.1 ±0.3	3.4 ±0.6	0.08	0.15
	117.5	3.2 ±0.4	5.7 ±0.8	0.30	0.34
	122.5	2.6 ±0.4	5.0 ±0.7	0.56	0.56
	127.5	3.5 ±0.5	7.1 ±0.9	0.86	0.89
	132.5	2.7 ±0.4	5.0 ±0.7	1.28	1.20
82°/40°	77.5	0.44 ±0.13	2.4 ±0.7	0.49	0.52
	82.5	0.38 ±0.12	2.2 ±0.7	0.33	0.37
	87.5	0.44 ±0.13	2.6 ±0.8	0.16	0.22
	92.5	0.87 ±0.19	5.4 ±1.2	0.05	0.14
	97.5	0.58 ±0.16	3.5 ±1.0	0.23	0.29
	102.5	0.78 ±0.18	4.7 ±1.1	0.43	0.45
	107.5	1.13 ±0.23	6.9 ±1.4	0.65	0.67
	112.5	0.51 ±0.15	3.1 ±0.9	0.90	0.93
	117.5	0.80 ±0.20	5.0 ±1.2	1.19	1.17
	122.5	1.75 ±0.29	10.3 ±1.6	1.57	1.56
102°/30°	72.5	0.18 ±0.09	1.9 ±1.0	0.09	0.17
	77.5	0.33 ±0.12	3.8 ±1.4	0.09	0.17
	82.5	0.33 ±0.12	4.5 ±1.7	0.28	0.33
	87.5	0.02 ±0.07	0.4 ±1.2	0.47	0.51
	92.5	0.11 ±0.07	2.3 ±1.4	0.68	0.71
	97.5	0.13 ±0.07	4.0 ±2.3	0.91	0.93
	102.5	0.20 ±0.09	5.8 ±3.	1.15	1.17
	107.5	0.13 ±0.08	3.8 ±2.	1.44	1.47
	112.5	0.27 ±0.13	7.0 ±3.	1.78	1.81
	117.5	0.52 ±0.17	8.8 ±3.	2.29	...

difference persists when the E_b cut between the states is varied $\pm\frac{1}{2}$ MeV.

In graphing $P(q)$ we have plotted a point to the right or left of $q=0$ according to which side of the nominal q versus T_p curve [Fig. 1(a)] that kinematic "bin" lay on. For small q values this choice is quite arbitrary, since it corresponds to the direction of the initial cluster momentum which, due to experimental resolution effects, is not well determined.

On the $P(q)$ for ground-state events we have superimposed the predicted distribution of Balashov,[10] arbitrarily normalized and flattened as it would be by the experimental resolution (but not shifted along the q axis). By comparison with this curve the experimental points appear to be "stretched" to higher T_p values, much as the angular distributions observed in $(p, 2p)$ experiments[13] are stretched towards larger angles. The two effects are kinematically equivalent,[26] and both might be due to refraction of the outgoing particles at the nuclear surface.

There is a striking difference in form between the ground- and first-excited-state momentum distributions; of course the disparity between the different angular configurations in the latter case raises the question whether knockout mechanism dominates, and whether this may be regarded as a momentum distribution at all. Recalling the 2^+ assignment of the 2.9-MeV state, one might ask whether the observed $P(q)$ could correspond to knockout of d-state clusters, shifted by refraction effects and filled in by experimental resolution. Monte Carlo studies show that so much filling in is not possible if the assumed d-state oscillator parameter is similar to the s-state parameter. The results at 102/30 show (statistically weak) evidence of a dip, not far from the q value of the s-state maximum, but this is contradicted by the other results. We cannot, therefore, draw any firm conclusions from these events, and further experimental studies should prove very interesting.

The shape of the ground-state $P(q)$ is not inconsistent with the early results of Samman and Cuer[1] and James and Pugh.[2] It has been usual in knockout experiments to fit $P(q)$ with analytic functions, obtaining parameters such as characteristic momenta, etc. The distortions evident even in the ground-state results show that such a procedure

would not be meaningful here and that, instead, some attempt to fit the data with a distorted-wave theory should be made.

C. Effective Number of α Clusters in Carbon

Let I(g.s.) and I(1st ex.) represent the integrals,

$$I \equiv \int_{-\infty}^{\infty} P(\vec{q})d\vec{q} = 4\pi \int_{0}^{\infty} P(q)q^2 dq ,$$

carried out over the experimentally measured ground state and first excited state $P(q)$, respectively. *If absorption of incoming and/or outgoing particles were negligible*, these integrals would be equal to the "effective number of α clusters" in carbon coupled to the ground and first excited states of Be^8, and their ratio could be directly interpreted as a coefficient of fractional parentage. Balashov, Boyarkina, and Rotter[10] have calculated a reduced width $\theta^2 = 0.542$ for an α cluster coupled to the ground state, and 0.677 for one coupled to the first excited state; the ratio 1st ex./g.s. is 1.25. The corresponding predictions of Beregi *et al.*[11] are 0.675 (g.s.) and 0.84 (1st ex.); the ratio is again 1.25. (In the latter case we have included only the α particles formed from the p^4 configuration of carbon, as did Balashov.) The slight discrepancy between calculations is insignificant compared to the uncertainty introduced by the absorption.

Since the knockout mechanism certainly seems valid for the g.s. events, we can attempt to compare I(g.s.) with the predictions. To evaluate I(g.s.), one must heuristically "correct" Fig. 9(a) for the distortions due to secondary interactions by arbitrarily shifting the origin of q to the point of maximum $P(q)$; doing this, and averaging over all our data we obtain

$$I(\text{g.s.}) = 0.13 \pm 50\% .$$

Since we know from $(p, 2p)$ experiments[13] that the reduction factor due to absorption for the incident and outgoing protons alone must be about 4, this value does not really seem low compared to the predicted[10,11] value of 0.6 or so; in fact it leaves little over for α absorption.

James and Pugh[2] however found (in our notation)

$$I(\text{g.s.}) + I(\text{1st ex.}) = 0.02^{+0.02}_{-0.01}$$

a value five times smaller than ours at the slightly lower incident energy 150 MeV. This disagreement is traceable to a disagreement in the absolute cross section. So large an effect is not due to experimental resolution differences,[27] nor is absorption expected to vary this rapidly with energy. The absolute cross section is of importance in checking any distorted-wave theory that may be advanced. Therefore, until the question is definitively settled by a third experiment, we would like to advance a somewhat indirect argument in favor of our value. The recent measurement by Roos *et al.*[5] of α knockout from Be^9 at 57 MeV yielded I(g.s.) = 0.26 (our notation) for that target – in exact agreement with the value we obtained[28] at 160 MeV, using the same counters, monitor, etc., as used here. This fact, taken at face value, implies a negligible difference in absorption at 57 and 160 MeV! If, on the other hand, absorption decreases with increasing energy as expected, this comparison with Ref. 5 indicates that our measurements err (if at all) in being too low, certainly not too high.

D. Ratio of Be^8 First-Excited to Ground State

The shape of $P(q)$ for the first-excited-state events [Fig. 9(b)] and our general doubts concerning the applicability of a knockout mechanism to these events would make computation of I(1st ex.) a meaningless exercise. However, the ratio of raw cross sections, appropriately weighted by statistical accuracy, averaged over all the data in the table is

$$d\sigma(\text{1st ex.})/d\sigma(\text{g.s.}) = 0.6 \pm 0.1 .$$

We have included in the error an estimate of the uncertainty due to the probable error in the E_b cut between the states. Therefore it appears that the first excited state is less populated than the ground state, rather than somewhat more populated as predicted.[10,11] This point is the more interesting in that absorption effects should largely cancel out. Of course the ratio I(1st ex.)/I(g.s.) would differ from the cross-section ratio because of the q^2 weighting, but a rather large effect would be required to bring experiment and theory into line.

We must note that Samman and Cuer[1] found a cross-section ratio

$$\sigma(\text{1st ex.})/\sigma(\text{g.s.}) = 6 .$$

This may not be an experimental contradiction, however. Their experiment, though at a high incident energy, involved proportionately far more low-energy outgoing α particles, which are produced in abundance by sequential decay. If the first excited state is strongly populated by sequential decay or secondary collisions, the ratio of first-excited- to ground-state events might depend strongly on the energy of the emitted α particles.

V. CONCLUSIONS

These measurements of quasi-elastic proton-α scattering in a variety of final-state configurations confirm the usefulness of the plane-wave impulse-approximation formula in interpreting the cross sections, even over a wide range of the proton-α interaction. The distortions, presumably due to secondary interactions, are certainly not negligible; however, the distorted momentum distribution, because of the ease with which it may be calculated from the data, seems a good meeting ground for different experiments, and for experiment with theory. The ratio of integrals of $P(q)$ for different states of the residual nucleus can be interpreted as parentage coefficients only if one is confident that such states arise from knockout rather than multiple processes; there is considerable doubt in the present case. The meaningful interpretation of the absolute cross section in terms of the effective number of α clusters in the target must await a satisfactory distorted-wave theory.

It is pleasure to thank Professor Karl Casper who furnished us with the deep solid-state detectors used in these measurements and who collaborated in later runs. Thanks are also due to Valdis Kirsis who helped take data, K. H. Wang who wrote most of the on-line computer programs, and Andreas M. Koehler and the cyclotron staff for their constant cooperation. One of us (BG) is deeply indebted to Harvard University for an appointment which made this and other experiments at the cyclotron possible.

APPENDIX

Derivation of the PWIA Formula

We derive the PWIA expression [Eq. (5)] for the knockout cross section, neglecting secondary interactions, relativistic effects, spin and off-energy-shell effects in the p-cluster interaction, but retaining those effects due to the finite mass of the residual nucleus. Accordingly, our target nucleus of mass A is represented as a structureless cluster (mass a, coordinate $\vec{r}_a$, initial and final wave vectors $\vec{k}_a, \vec{k}_a'$) bound to a "core" [mass $(A-a)$, coordinate $\vec{r}_c$, wave vectors $\vec{k}_c, \vec{k}_c'$]. The mass, coordinate, and initial and final wave vectors of the incident proton (or other particle) are m, $\vec{r}_0$, $\vec{k}_0$, and $\vec{k}_0'$.

We shall also use the coordinates

$$\vec{R} \equiv \vec{r}_0 - \vec{r}_a = \text{relative proton-cluster coordinate},$$

$$\vec{S} \equiv \vec{r}_c - \vec{r}_a = \text{relative core-cluster coordinate},$$

$$\vec{T} \equiv \frac{(A-a)\vec{r}_c + a\vec{r}_a}{A} = \text{coordinate of the c.m. of the target nucleus},$$

and shall define $\vec{Q}$ as the momentum conjugate to $\vec{S}$, and $\vec{P}$ as the momentum conjugate to $\vec{T}$ (namely, the initial momentum of the target nucleus). Then the relevant matrix element is

$$\langle f|U|i\rangle = V^{-5/2}\iiint d\vec{r}_0 d\vec{r}_a d\vec{r}_c \; e^{-i\vec{k}_0'\cdot\vec{r}_0} e^{-i\vec{k}_a'\cdot\vec{r}_a} \times e^{-i\vec{k}_c'\cdot\vec{r}_c} U(\vec{R})\; e^{i\vec{k}_0\cdot\vec{r}_0} e^{i\vec{P}\cdot\vec{T}} \Psi(\vec{S}).$$

Each wave function is normalized to a volume V. The final state is a product of three plane waves. The initial state is a product of a plane wave representing the incident proton, a plane wave describing the c.m. of the target nucleus, and a bound-state wave function in the relative coordinate of the cluster and core. We have taken as the only interaction some potential $U(\mathrm{R})$ between the incident proton and the cluster. Replacing $\Psi(\vec{S})$ by its Fourier integral representation

$$\Psi(\vec{S}) = (2\pi)^{-3/2}\int_{-\infty}^{\infty} d\vec{Q} e^{i\vec{Q}\cdot\vec{S}} \Phi(\vec{Q}),$$

rewriting the matrix element in terms of $\vec{R}$, $\vec{S}$, and $\vec{T}$; setting $\vec{P}=0$ (which puts the calculation in the laboratory system of coordinates) and integrating over $\vec{S}$ and $\vec{T}$ we obtain

$$\langle f|U|i\rangle = (2\pi)^{9/2} V^{-5/2}\iint d\vec{R} d\vec{Q}\, \Phi(\vec{Q})\; e^{-i\vec{k}_0'\cdot\vec{R}} U(\vec{R}) \times e^{i\vec{k}_0\cdot\vec{R}} \delta(\vec{k}_0 - \vec{k}_0' - \vec{k}_a' - \vec{k}_c') \times \delta\left(\left(\frac{a}{A} - 1\right)(\vec{k}_0 - \vec{k}_0' - \vec{k}_a') - \frac{a}{A}\vec{k}_c' + \vec{Q}\right).$$

To integrate over $\vec{Q}$ we replace the argument of Φ by

$$\vec{q} \equiv \frac{a}{A}\vec{k}_c' - \left(\frac{a}{A} - 1\right)(\vec{k}_0 - \vec{k}_0' - \vec{k}_a'),$$

and obtain

$$\langle f|U|i\rangle = (2\pi)^{9/2} V^{-5/2}\int d\vec{R}\, e^{-i\vec{k}_0'\cdot\vec{R}} U(\vec{R}) \times e^{i\vec{k}_0\cdot\vec{R}}\, \Phi(\vec{q})\delta(\vec{k}_0 - \vec{k}_0' - \vec{k}_a' - \vec{k}_c').$$

In time-dependent perturbation theory, the cross section is given by

$$d\sigma = \frac{|\omega_{i\to f}|^2}{\tau \times |\text{incident flux}|} \times \begin{pmatrix}\text{final-state}\\ \text{phase space}\\ \text{volume element}\end{pmatrix},$$

where τ is an arbitrary time interval, long compared to the interaction time, and $\omega_{i\to f}$ is the transition amplitude

$$\omega_{i\to f} = -\frac{i}{\hbar}\int_{-\tau/2}^{+\tau/2} dt\langle f|U|i\rangle e^{i[(E_f - E_i)/\hbar)t]} .$$

E_i and E_f are initial- and final-state energies. The phase-space volume element is

$$\frac{Vd\vec{p}_0'}{(2\pi\hbar)^3}\times\frac{Vd\vec{p}_a'}{(2\pi\hbar)^3}\times\frac{Vd\vec{p}_c'}{(2\pi\hbar)^3} ,$$

where $p=\hbar\vec{k}$ stands for a momentum, and the incident flux is

$$\left|\frac{\hbar}{2mi}(\Psi^*\nabla\Psi - \Psi\nabla\Psi^*)\right| = \frac{\hbar}{m}\frac{k_0}{V} .$$

Putting the last five equations together, integrating over time in the transition amplitude, and using the usual rules such as

$$\delta^2(E) = \delta(0)\delta(E) = \frac{\tau}{2\pi}\delta(E)$$

for reducing squared δ functions, we obtain

$$d\sigma = \frac{(2\pi)^{-2}m}{\hbar^2 k_0}\,\delta(E_f - E_i)\delta(\vec{k}_0 - \vec{k}_0' - \vec{k}_a' - \vec{k}_c')$$

$$\times P(\vec{q})|U'(\vec{k}_0 - \vec{k}_0')|^2 d\vec{k}_0' d\vec{k}_a' d\vec{k}_c' ,$$

where $U'(\vec{k}_0 - \vec{k}_0') \equiv \int dR\, e^{-i\vec{k}_0'\cdot\vec{R}}\, U(R)\, e^{i\vec{k}_0\cdot\vec{R}}$,

and $P(\vec{q}) \equiv |\Phi(\vec{q})|^2$ = probability density distribution of $\vec{q}$.

We must now integrate over a momentum and an energy to obtain a quantity which can be compared with experiment. Choosing first the momentum $\vec{k}_c'$ (since it is not observed in the experiment) we obtain

$$d\sigma = \frac{(2\pi)^{-2}m}{\hbar^2 k_0}\,\delta(E_f - E_i)P(\vec{q})|U'(\vec{k}_0 - \vec{k}_0')|^2 d\vec{k}_0' d\vec{k}_a' ,$$

where we now have

$$\vec{q} = \frac{a}{A}(\vec{k}_0 - \vec{k}_0' - \vec{k}_a') - \left(\frac{a}{A} - 1\right)(\vec{k}_0 - \vec{k}_0' - \vec{k}_a') ,$$

$$= \vec{k}_0 - \vec{k}_0' - \vec{k}_a' ,$$

= final momentum of the residual nucleus.

But $\vec{q}$ is also the initial momentum of the "core" (since by hypothesis it did not participate in the reaction) and therefore, since the (core + cluster) system was initially at rest in the laboratory, $-\vec{q}$ is the initial momentum of the cluster in the laboratory. Any "secondary" interactions (and these certainly occur in nature) will tend to destroy this convenient interpretation of $\vec{q}$.

We must still integrate over the energy-conserving δ function. To omit this step, as is sometimes done, is inadvertently to disregard the effect on the cross section due to the recoil of the residual nucleus. Using the relation

$$\int \delta\Big(g(x)\Big)h(x)dx = \sum_i \frac{h(x_i)}{|g'(x_i)|}$$

[where x_i are the roots of $g(x)=0$] to integrate over $|\vec{k}_a'|$, we obtain:

$$d\sigma = \frac{(2\pi)^{-2}}{\hbar^4} ma\frac{k_a'}{k_0} f P(\vec{q})|U'(\vec{k}_0 - \vec{k}_0')|^2 d\vec{k}_0' d\Omega_a' ,$$

where

$$f = \left(1 - \frac{a}{A}\right)\left[1 + \frac{a}{A}\left(\frac{k_0'}{k_a'}\cos(\theta_p + \theta_a) - \frac{k_0}{k_a'}\cos\theta_a\right)\right]^{-1}$$

in our geometry; we assume the reaction is coplanar and θ_p, θ_a are the outgoing proton and cluster angles measured to the beam direction. For large A, $f \to 1$.

Now $U'(k_0 - k_0')$ is the same matrix element as appears in the Born approximation formula for free proton-α scattering in the c.m. frame:

$$\left(\frac{d\sigma}{d\Omega}\right)_{p\alpha,\,\mathrm{c.m.}} = \frac{(2\pi)^{-2}}{\hbar^4}\left(\frac{ma}{m+a}\right)^2 |U'(\vec{k}_0 - \vec{k}_0')|^2 ,$$

if we neglect the off-energy-shell effects in the three-body case. Doing this, and also setting

$$d\vec{k}_0' = \frac{m}{\hbar^2} k_0' dT_0' d\Omega_0' ,$$

we finally obtain

$$\frac{d\sigma}{dT_0' d\Omega_0' d\Omega_a'} = \frac{m}{\hbar^2}\frac{(1 + a/m)^2}{a/m}\frac{k_0' k_a'}{k_0} f\left(\frac{d\sigma}{d\Omega}\right)_{p\alpha,\,\mathrm{c.m.}} P(\vec{q})$$

the same, except for slight differences in notation, as Eq. (5) of the text.

*Work supported by the Office of Naval Research and National Science Foundation Grant No. GP-9217.

[1]A. Samman and P. Cuer, J. Phys. Radium 19, 13 (1958).

[2]A. N. James and H. G. Pugh, Nucl. Phys. 42, 441 (1963).

[3]C. Ruhla *et al.*, Phys. Letters 6, 282 (1963).

[4]T. Yuasa and E. Hourani, Rev. Mod. Phys. 37, 399 (1965).

[5]P. G. Roos *et al.*, Phys. Rev. 176, 1246 (1969).

[6]M. Epstein *et al.*, Phys. Rev. 178, 1698 (1969).

[7]V. I. Komarov, G. E. Kosarev, and O. V. Savchenko, Joint Institute for Nuclear Research, Dubna, 1969 (to be published).

[8]D. F. Jackson, Rev. Mod. Phys. 37, 393 (1965).

[9]D. F. Jackson, Nuovo Cimento 40B, 109 (1965). Our 102/30 configuration is similar to the "medium-energy" experiment proposed by Jackson.

[10]V. V. Balashov, A. N. Boyarkina, and I. Rotter, Nucl. Phys. 59, 417 (1964).

[11]P. Beregi *et al.*, Nucl. Phys. 66, 513 (1965).

[12]Y. Sakamoto, Nucl. Phys. 66, 531 (1965).

[13]B. Gottschalk, K. H. Wang, and K. Strauch, Nucl. Phys. A90, 83 (1967).

[14]In contrast to this more specific meaning, quasifree is sometimes used synonymously with quasi-elastic.

[15]M. Riou, Rev. Mod. Phys. 37, 375 (1965).

[16]A. M. Cormack *et al.*, Phys. Rev. 115, 599 (1959). The absolute cross section given in their Table II should be increased 11% [see J. N. Palmieri *et al.*, Phys. Letters 6, 289 (1963)]. Also, the lab-to-c.m. conversion in that table is not quite correct; Professor Palmieri was kind enough to supply us with the correct conversion factor.

[17]M. Rich and R. Madey, University of California Radiation Laboratory Report No. UCRL-2301 (unpublished).

[18]Harshaw Chemical Co., Cleveland, Ohio, Model 12S. This "integral line" counter had been specially selected for uniformity of response over its volume, and by itself had 0.8% FWHM line width at 154 MeV.

[19]Ortec Inc., 100 Midland Road, Oak Ridge, Tennessee, Model 100-100.

[20]This detector was made by Professor Karl Casper of Cleveland State University. The correction ranges from 5 to 16%.

[21]However, we would like to acknowledge some recent conversations with Professor H. G. Pugh who independently evolved a treatment similar to ours. His numerical results and ours, for instance in the James and Pugh geometry (Ref. 2), are in good agreement.

[22]The distorted momentum distribution $P(q)$ is "distorted" for two reasons: (a) nuclear effects such as secondary interaction, and (b) the experimental resolution effects. In any knockout experiment, we must be certain that distortions attributed to nuclear effects are not in fact due to the experiment.

[23]We have not corrected our results for this effect which was at worst comparable to the statistical uncertainty.

[24]To be more precise, it is 30% lower if the datum is plotted at the nominal q value for that bin, i.e., $q=0$. If we plot it at the *most likely* q value (0.15 fm^{-1}) the discrepancy between the "measured" and "true" distributions is reduced to 10%.

[25]D. F. Measday, Nucl. Instr. Methods 34, 353 (1965).

[26]One can argue as follows: Suppose some agency – presumably refraction at the nuclear surface – deflects the outgoing proton to a larger angle. It will then have a greater energy at a given angle of observation.

[27]The finite-counter effect in the James and Pugh experiment was about 20% according to H. G. Pugh (private communication) and our own Monte Carlo calculation using the appropriate parameters.

[28]S. L. Kannenberg, Ph.D. thesis, Northeastern University (unpublished); B. Gottschalk, S. L. Kannenberg, and K. Casper, to be published.